

NANOSCALE INVESTIGATION OF VARIOUS MAGNETITE MORPHOLOGIES IN THE SAMPLES RETURNED FROM C-TYPE ASTEROID RYUGU: INSIGHTS INTO THE AQUEOUS ALTERATION PROCESSES. E. Dobrică¹, H. A. Ishii¹, J. P. Bradley¹, K. Ohtaki¹, T. Noguchi^{2,3}, H. Yurimoto⁴, T. Nakamura⁵, H. Yabuta⁶, H. Naraoka⁷, R. Okazaki⁷, K. Sakamoto⁸, S. Tachibana⁹, S. Watanabe¹⁰, Y. Tsuda⁸, and the Min-Pet Fine Sub-team. ¹Hawai'i Institute of Geophysics and Planetology, School of Ocean, Earth Science, and Technology, University of Hawai'i at Mānoa, Honolulu, HI (dobrica@hawaii.edu), ²Division of Earth and Planetary Sciences, Kyoto University; Kyoto, Japan. ³Faculty of Arts and Science, Kyushu University, Fukuoka, Japan. ⁴Department of Earth and Planetary Sciences, Hokkaido University, Sapporo, Japan. ⁵Department of Earth Science, Graduate School of Science, Tohoku University, Sendai, Japan. ⁶Earth and Planetary Systems Science Program, Hiroshima University, Hiroshima, Japan. ⁷Department of Earth and Planetary Sciences, Kyushu University, Fukuoka, Japan. ⁸Institute of Space and Astronautical Science, Japan Aerospace Exploration Agency, Sagami-hara, Kanagawa, Japan. ⁹UTokyo Organization for Planetary and Space Science, University of Tokyo, Tokyo, Japan. ¹⁰Department of Earth and Environmental Sciences, Nagoya University, Nagoya, Japan.

Introduction: Samples returned from the carbonaceous asteroid 162173 Ryugu by the JAXA Hayabusa2 mission allow us to investigate primitive materials of our Solar System and their evolution [1-2]. The Ryugu samples are composed of minerals similar to those of CI (Ivuna-like) carbonaceous chondrites indicating that the parent planetesimal from which Ryugu was derived experienced severe aqueous alteration [1].

Magnetite is the most abundant coarse-grained constituent of CI chondrites (3–5 vol%), and it occurs as framboids, plaquettes, spherules, and irregularly shaped grains [3]. They are products of alteration, and their formation is controlled by nucleation during aqueous alteration on the parent body [4]. We investigate the presence of magnetite in the Ryugu sample because it can provide important information about the evolution of the aqueous alteration processes on the carbonaceous (C-type) asteroids.

Methods: One FIB section (A0104-00200201) was studied using a variety of TEM techniques, including scanning transmission electron microscopy (STEM) imaging, nanodiffraction, and energy-dispersive X-ray spectroscopy (EDS). All imaging and analysis were carried out at 300 kV using the Titan G2 analytical (S) TEM at Advanced Electron Microscopy Center (AEMC) at the University of Hawai'i at Mānoa. Crystalline phases were identified by electron nanodiffraction and EDS. Nanodiffraction was carried out using a camera length of 295 mm and a convergence angle of 0.3 mrad. Additional EDS hyperspectral maps were collected at the Molecular Foundry, Lawrence Berkeley National Laboratory using a 80–300 kV TitanX “ChemSTEM” with four windowless X-ray silicon drift detectors (0.7 sr solid angle).

The elemental compositions of carbonates reported here were extracted from EDS mapping over areas of 5–10 nm (at the Molecular Foundry). The EDS maps were

collected at 200 kV and displayed using the Esprit 1.9 software package (Bruker Corporation) as color-coded maps. Compositions were normalized to 100%. The EDS detection limit for the TEM measurements is estimated to be <0.1 wt%. Oxygen abundances should be viewed with caution because oxygen K X-rays are subject to variable amounts of self-absorption by the sample.

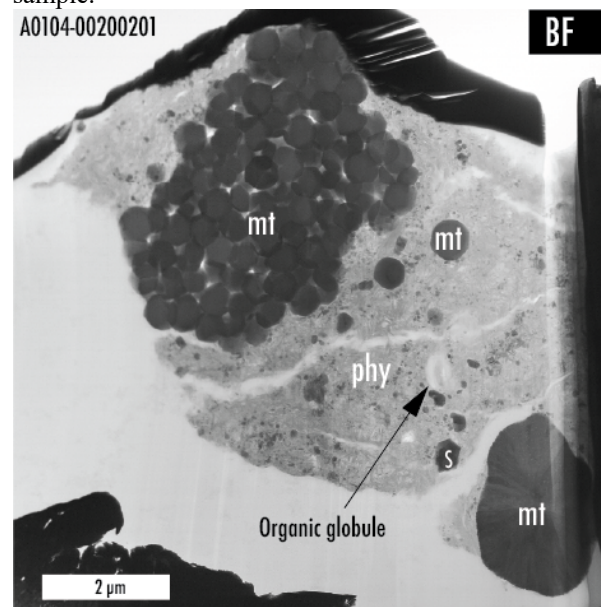


Figure 1. Bright-field (BF) STEM image of the FIB section analyzed in this study (A0104-00200201) showing the presence of framboidal and spherical magnetite (mt), euhedral sulfides (S), and an organic globule embedded in a coarse-grained matrix of phyllosilicates (phy).

Results and discussion: Detailed TEM observations of the FIB section, A0104-00200201, show the presence of magnetite, Ni- and Co-rich sulfides, and an organic globule (430 x 630 nm in size) embedded in a groundmass that consists of coarse-grained phyllosilicates (Fig. 1).

Magnetite with three different morphologies was identified in this FIB section: (1) framboidal clusters, (2) single dodecahedrons embedded in the fine-grained matrix, and (3) spherulitic aggregates of magnetite (Figs. 1-2). The framboidal aggregate is $\sim 3 \times 5.3 \mu\text{m}$ in size, the crystals embedded in the fine-grained matrix have sizes up to $0.6 \times 0.6 \mu\text{m}$, and the spherulite magnetite is $\sim 2.9 \mu\text{m}$ in length and $\sim 2 \mu\text{m}$ wide. We focus on the spherulite magnetite grain that contains numerous nanometric euhedral to subhedral pores. Their sizes vary from a few nanometers up to $\sim 45 \text{ nm}$ in length, and they are homogeneously distributed in the spherulite aggregate. The pores are absent in the framboidal and the single dodecahedrons magnetite coexisting in close proximity. Figure 2 shows the spherulite aggregate of magnetite and reveals the internal texture showing clear individual radiating fibers. The adjacent fibers have an epitaxial relationship. The surface of the spherulite magnetite shows euhedral laths of the radiating fibers, with laths up to $\sim 50 \text{ nm}$ wide. No clear evidence of space weathering was observed in the magnetite crystals identified in this FIB section.

These microstructural features can provide important information about the evolution history of the aqueous alteration processes on the Ryugu asteroid. Lofgren [5] suggested that spherulites develop wherever the growth rate (G) is higher than diffusion rate (D , $G \gg D$). The transition in crystal habits is related to variation in D/G ratio [5]. The presence of magnetite with varying crystal habits in the Ryugu samples suggests a variable range of growth and diffusion rates on the parent body. Further TEM analysis will focus on the presence and the formation of the euhedral pores in the spherulite magnetite.

Conclusion: In this study, we describe the microstructural differences between different magnetite morphologies, which could result from the chemical conditions (growth vs. diffusion rate) that existed during their formation.

Acknowledgments: Work at the Molecular Foundry was supported by the Office of Science, Basic Energy Sciences, and the U.S. Department of Energy.

References: [1] Noguchi T. et al. (2022) *53rd LPSC*, this volume. [2] Tachibana S. (2021) *Sample Return Missions the Last Frontier of Solar System Exploration*, Chapter 7, Elsevier, Editor Longobardo A., 147-162. [3] Alfing J. et al. (2019) *Geochemistry*, 79, 125532. [4] Kerridge J. F., et al. (1979) *Science*, 205, 395-397. [5] Lofgren G. (1974) *Americ. J. Sci.* **274**, 243-273.

Figure 2 (right column). Bright-field STEM (a-b) and high-resolution (HR, c) images show the texture of the spherulitic magnetite (mt) and the associated minerals

phases. b) Euhedral (black arrows) to anhedral pores are homogeneously distributed in the magnetite. c) Euhedral laths at the surface of the spherulitic magnetite grain. Other phases identified: S – sulfide, and phy – phyllosilicate.

